2.33. ELECTROCHEMICAL POLARIZATION STUDIES OF API 5L GRADE X65 STEEL IN CHLORIDE SOLUTION

B. Mazza[1], T. Pastore[1], P. Pedeferri[1], and G. Rondelli[2]

1. Dipartimento di Chimica Fisica Applicata, Politecnico di Milano, Italy
2. Istituto per la Tecnologia dei Materiali Metallici non Tradizionali, CNR, Cinisello Balsamo (MI), Italy

ABSTRACT

Anodic and cathodic polarization measurements were carried out in 3.5% NaCl solution on API 5L grade X65 steel commonly used for offshore structures. Tests were performed on a rotating disk electrode and both potentiodynamic and potentiostatic polarization methods were employed. An analytical expression for the polarization curve is proposed to describe boundary conditions on the cathode for current and potential distribution calculations. The parameters of this expression are discussed and obtained directly from experimental polarization curves.

INTRODUCTION

During the last few years, mathematical modelling of current and potential distribution has been widely studied to improve design methods for the cathodic protection of offshore structures. For this purpose, several numerical methods have been proposed to calculate the distribution on the surface of complex structures such as offshore ones [1-3].

The distribution can be obtained resolving the Laplace equation in the environment surrounding the structure and imposing that the solution satisfies the boundary conditions. On the surface of the anodes and of the structure, such conditions relate the metal/environment potential to the circulating current density and coincide with polarization curves of the materials.

On anodic materials, simplified conditions derived from the characteristics of the cathodic protection system are taken into account. So, for impressed current systems the value of the current is imposed on anodes, while sacrificial anodes can be assumed to operate at constant potential (non polarizable anodes).

In order to assign the boundary conditions on the structure, usually made of carbon and mild steels, it is necessary:

i) to describe the polarization curve by an analytical expression ,

ii) to determine the influence of the various environmental factors on the polarization curve and to predict its time dependence.

Then, current and potential distribution calculation requires an accurate evaluation of the polarization characteristics of carbon steel in sea water. This cannot be obtained nowadays due to the lack of sufficiently reliable experimental data. Moreover, general improvement of design methods for cathodic protection also calls for such better evaluation.

The electrochemical behaviour of iron and, to a lower extent, of steels has been widely studied in the past, but few data are available on the polarization curves in chloride solutions with pH values similar to that of sea water |4| or higher than 3 |5|. Furthermore, there is a lack of data in sea water. In this environment, owing to the formation of a calcareous deposit, the study of the polarization curves is more difficult because of the time dependence of the curves themselves. With regard to this, some models taking into account the effect of the deposit growth have been recently proposed |6,7| just to define the boundary conditions.

The aim of this work was to define the boundary conditions in order to estimate current and potential distribution on a cathodically protected structure. It is part of a systematic research carried out with the collaboration of Tecnomare, Snamprogetti and Agip to develop new design methods for cathodic protection of offshore structures. In particular, the cathodic behaviour of a structural steel in the absence of any calcareous deposit was studied to check the effectiveness of a mathematical model |8|. The data obtained can be considered to maintain a certain validity also for a real structure during the initial polarization in sea water, when calcareous deposits are not yet formed.

ANALYTICAL EXPRESSION OF THE POLARIZATION CURVE

The polarization curve has the typical shape shown in Fig. 1. Such curve

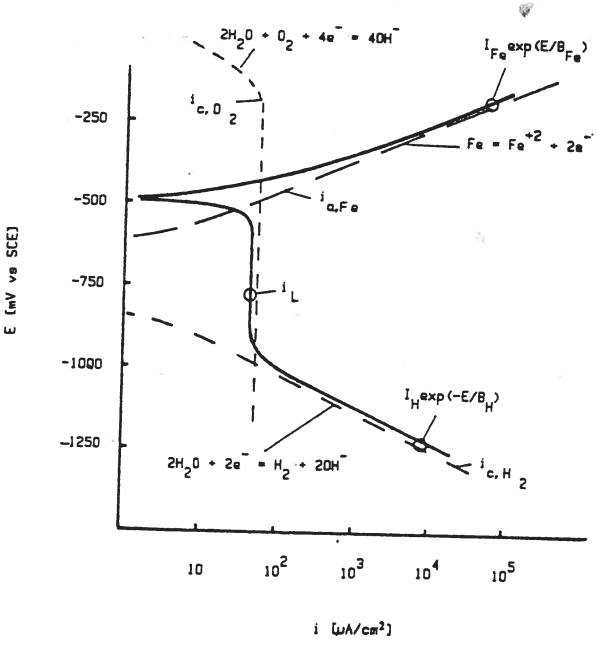

Fig. 1 - Representative polarization curve(solid line) and partial reactions for Fe in aerated 35 g/l NaCl.

results from three processes: the anodic metal dissolution and the cathodic reactions of oxygen reduction and hydrogen evolution. Assuming that the partial processes occur uniformly and independently and summing the respective currents, the polarization curve can be mathematically represented by the expression |9|:

$$i = I_{Fe}\exp(E/B_{Fe}) - i_L - I_H\exp(-E/B_H) \quad (1)$$

where the contributions of the three processes are written supposing that both the steel dissolution and the hydrogen evolution occur according to Tafel law and the oxygen reduction takes place under limiting current conditions so that its rate can be simplified as a constant term, i_L. Other expressions have also been suggested |10-12|.

Owing to the complexity of biological, chemical and physical phenomena involved, it is impossible to evaluate theoretically the parameters of above expression in natural environment, but they should be obtained as described in Fig. 1 from field data of polarization curves. However, under simplified conditions the parameters necessary to describe the curve can be obtained from literature data and laboratory tests. So, for sandblasted or pickled and not precorroded steel, that is in the absence of any surface deposit, the following values are reported for steel dissolution in chloride solution |4|:

$$I_{Fe} = 1.5\times10^{7}\ A/cm^2\ ,\quad B_{Fe} = RT/F \quad mV$$

(the temperature is in °K, and the potential in Eq.(1) is referred to the saturated calomel electrode, SCE). The expression given for B_{Fe} corresponds to a Tafel slope of about 60 mV/decade at 20°C. These parameter values have been obtained in 0.1÷1.5M NaCl solutions, with pH values ranging between 3 and 8.5 and temperatures between 19 and 23°C. Furthermore, for hydrogen evolution the following values, obtained in 0.1÷4M NaCl solution with pH ranging from 5 to 10 and at temperatures between 19 and 23°C, are reported |4|:

$$I_H = 8\times10^{-14}\ A/cm^2$$

$$B_H = RT/0.5F\ mV\ (\text{Tafel slope}\cong 120\ mV/\text{decade})$$

For potentials more negative than -1100 mV (SCE) or pH values higher than 10 the Tafel slope increases up to 140÷165 mV/decade (at 20°C) |4|. Elsewhere, values of 174 mV/decade are reported |5|.

In the absence of any deposits, the oxygen limiting current density mainly depends on convective oxygen mass transport to the metallic surface and hence it depends on environment velocity, oxygen content, temperature, etc. So, this parameter can be theoretically figured out only for simple geometries by means of expressions usually given in terms of dimensionless numbers, whereas generally it must be obtained experimentally. In the work by Selman and Tobias |12| several expressions for the limiting current density calculation are reported.

EXPERIMENTAL METHOD

Tests were carried out on a rotating disk electrode made of C-Mn steel type API 5L grade X65, commonly used for offshore structures, with composition in wt %: C 0.07, Mn 1.57, Si 0.28, P 0.019, S 0.011, Al 0.027, Nb 0.05, Cu 0.012, Cr 0.22. Tests were conducted at temperatures between 10 and 23°C in both aerated and deaerated 35 g/l NaCl solution with pH 8.2 (that is equal to the pH of synthetic sea water), using an electrochemical cell similar to that of the ASTM G5-82 procedure, slightly modified to contain more solution (2 l). A saturated calomel reference electrode and a platinum counter electrode were employed. The steel electrode was abraded to 1000 mesh finish using emery paper, washed with distilled water and degreased with acetone. Before the test, at least 1.5 l of solution were saturated in the cell by air or nitrogen bubbling for about one hour. Then the rotating disk electrode was introduced into the cell and the steel cathodically polarized for some minutes at -700 mV (SCE).

Two different types of tests were conducted:

i) potentiodynamic tests at a scanning rate of 10 mV/min and at a given rotation speed (4.3, 25, or 83 Hz),

ii) potentiostatic tests, in which steady state circulating current was measured at various rotation speeds (ranging from 0 to 83 Hz).

RESULTS AND DISCUSSION

Figures 2 to 4 show some potentiodynamic polarization curves.

The results of potentiostatic tests were transformed in terms of dimensionless numbers [12-13] by means of the following expressions:

$$\text{Sherwood number (Sh)} = \frac{i\,r}{nFDC}$$

$$\text{Reynolds number (Re)} = \frac{2\pi r^2 f}{\nu}$$

$$\text{Schmidt number (Sc)} = \frac{\nu}{D}$$

where r and f are the radius (11.1 mm) and the rotation frequency of the disk electrode, D and C the diffusion coefficient and the concentration of dissolved oxygen, and ν the kinematic viscosity. The values of the diffusion coefficient, concentration of oxygen dissolved in air saturated solution and kinematic viscosity were obtained interpolating literature data [14]. Some results expressed as dimensionless numbers for the steady state currents measured in potentiostatic tests as well as for the limiting currents obtained from potentiodynamic curves (flex points), are shown in Fig. 5.

From the results of the potentiostatic tests, it follows that at potentials ranging between -800 and -1000 mV (SCE) the Sherwood number is a linear function (in logarithmic scales) of the Reynolds number and of the Schmidt number. The experimental data agree quite well with the following theoretical expression va-

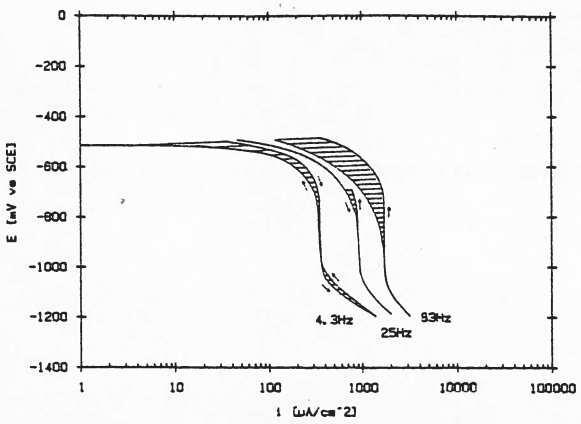

Fig. 2 - Potentiodynamic cathodic polarization curves for API 5L grade X65 steel rotating disk in aerated 35 g/l NaCl, pH 8.2, 20°C, rotation frequency as indicated.

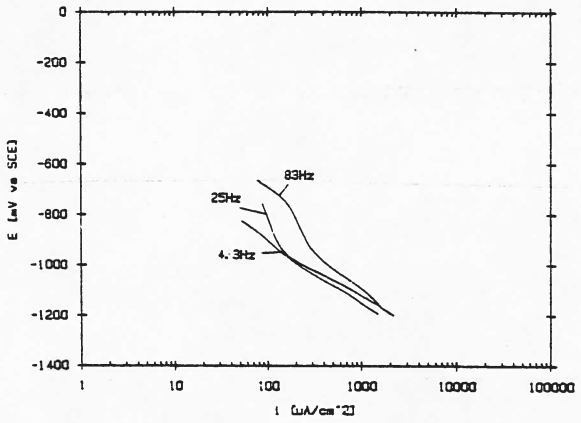

Fig. 3 - Potentiodynamic cathodic polarization curves for API 5L grade X65 steel rotating disk in deaerated 35 g/l NaCl, pH 8.2, 20°C, rotation frequency as indicated.

lid for the limiting current density [15]:

$$Sh = 0.621(1+0.298Sc^{-1/3}+0.14514Sc^{-2/3})^{-1} \cdot Re^{1/2}.Sc^{1/3} \qquad (2)$$

The measured current density, which in practice can be identified with the li-

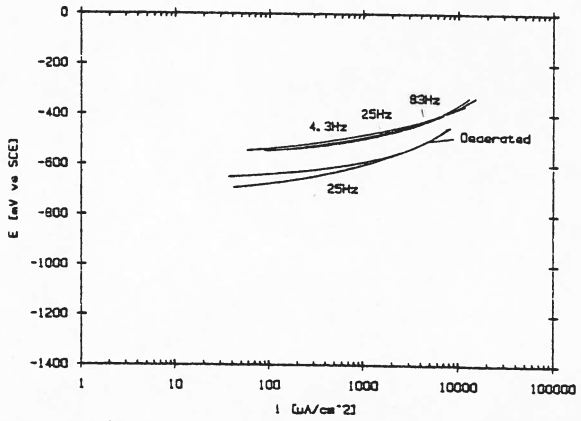

Fig. 4 - Potentiodynamic anodic polarization curves for API 5L grade X65 steel rotating disk in both aerated and deaerated 35 g/l NaCl, pH 8.2, 20°C, rotation frequency as indicated.

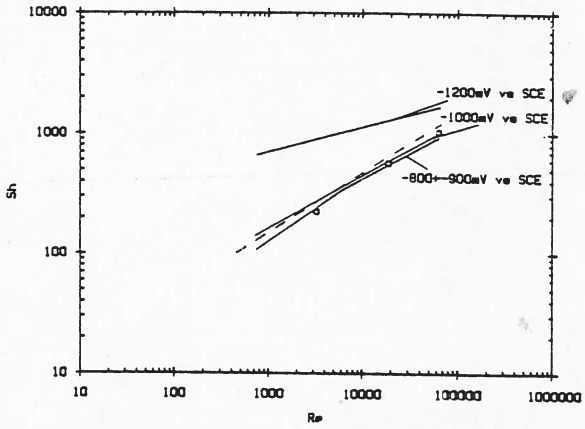

Fig. 5 - Relation between Sherwood number and Reynolds number for API 5L grade X65 steel rotating disk in aerated 35 g/l NaCl, pH 8.2, 20°C, Sc = 492.
(o) Limiting current density from potentiodynamic tests (flex points)
(—) Steady state current density in potentiostatic tests, potential as indicated
(--) Theoretical relation, Eq. (2)

miting current density at the considered potentials, increases one order of magnitude when rotation frequency increases from 0 to 83 Hz.

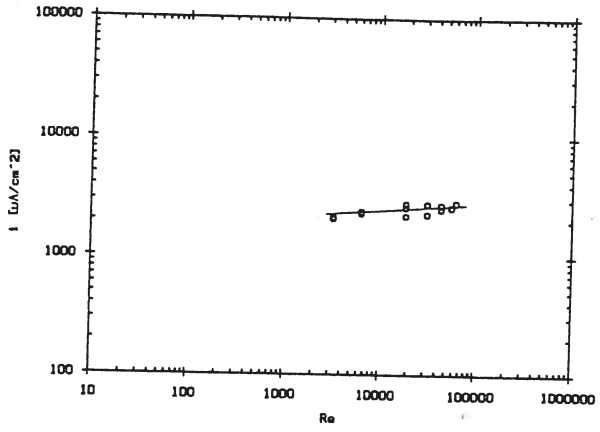

Fig. 6 - Relation between steady state current density in a potentiostatic test at -1200 mV (SCE) and Reynolds number for API 5L grade X65 steel rotating disk in deaerated 35 g/l NaCl, pH 8.2, 20°C.

The current density values measured at -1200 mV (SCE) are higher than the values obtained from Eq. (2) and those measured at more positive potentials, because the contribution of hydrogen evolution to circulating current is noticeable at -1200 mV. At this potential, the Reynolds number has a lower influence on the Sherwood number: so, the current density becomes only 4÷5 times higher when the rotation frequency increases from 0 to 83 Hz (Fig. 5). Moreover, under deaerated conditions the current density is not highly dependent on Re and it increases only twice when the frequency varies from 0 to 83 Hz (fig. 6). This slight increase could be mainly attributed to the experimental conditions adopted, owing to a low content of oxygen still present in the solution.

The results of the potentiodynamic tests are in good agreement with potentiostatic polarization data. The rotation speed affects the intermediate vertical branch of the polarization curve in correspondence to the oxygen limiting current (Fig. 2). At more negative potentials, the effect of the rotation speed decreases and the curves obtained at different rotation speeds approach each other. The difference between the curves observed at potentials more negative than -1000 mV (SCE) can be attributed also in this case to the effect on the oxygen limiting current; in fact, if the limiting current density is deducted (fig. 7), the remaining current density, due only to the hydrogen evolution, does not depend on the rotation speed. At more positive potentials, the anodic potentiodynamic curves (Fig. 4) do not vary with rota-

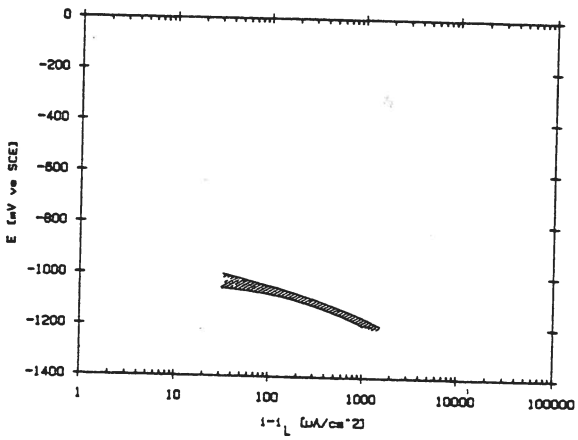

Fig. 7 - Current due to hydrogen evolution obtained after subtracting oxygen limiting current from total current of polarization curves (i=f(E)) reported in Fig. 2. Experimental conditions as in Fig. 2.

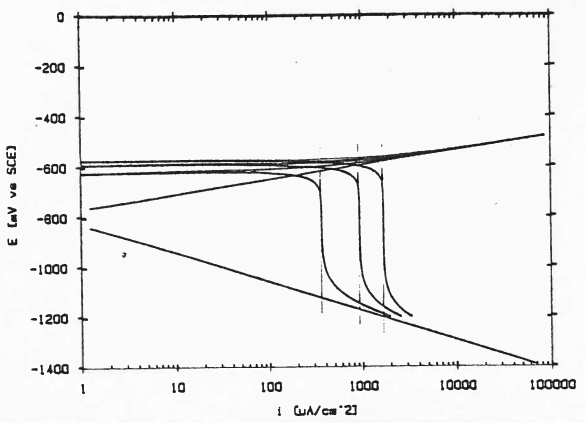

Fig. 8 - Cathodic polarization curves for API 5L grade X65 steel rotating disk in aerated 35 g/l NaCl, pH 8.2, 20°C, synthesized through Eq. (1) with limiting current from experimental curves of Fig.2.

tion speed, whereas the free corrosion potential seems slightly to increase.

Polarization curves calculated through Eq. (1), assuming the above-mentioned values for the I_{Fe}, B_{Fe}, I_H and B_H parameters and the limiting current densities resulting from the experimental curves of Fig. 2, are shown in Fig. 8. Moreover, this figure gives the three components of the total current (thin line). Comparing Fig. 2 with Fig. 8, the good agreement between the experimental and the theoretical curves for potentials more negative than -700 mV (SCE) has to be pointed out. At potentials more positive than -700 mV the polarization curve calculated on the basis of Eq. (1) deviates from the experimental curve. The measured free corrosion potential is 80 mV higher. This can be mainly attributed to the steel dissolution process. In fact, under aerated conditions and at current densities between about 100 and 1000 $\mu A/cm^2$, the experimental anodic polarization curves (Fig. 4) exhibit an exponential behaviour similar to that represented by the first term of Eq. (1), but the curves are shifted by 80 mV in the anodic direction. Only under deaerated conditions and after cathodic activation at -1200 mV (SCE) the experimental and the theoretical curves coincide (Figs. 4 and 8).

Turnbull and Gardner [4], taking into account also the work of other authors, suggest that oxide film formation occurs at potentials between -580 and -700 mV(SCE), especially at pH values higher than 10. At lower pH values the phenomenon is less evident, however it is appreciable at 8.5.

From the results of our tests, the free corrosion potential falls within the range in which the oxide film formation can occur. Moreover, under aerated conditions the simultaneous oxygen reduction reaction should facilitate the film or the corrosion products formation, which can hinder both the anodic and the cathodic reactions. Last, at such positive potentials the oxygen reduction is no more under limiting current conditions so that its rate cannot be simplified as a constant term i_L, but it must be represented by a more complex expression [9].

The comparison between Fig. 2 and Fig. 3 shows the effect of dissolved oxygen on the cathodic polarization curve. As the limiting current density decreases due to the reduction in the

oxygen concentration, the hydrogen evolution becomes evident at more positive potentials and the polarization curve is less influenced by the rotation speed. The experimental curves approach the Tafel stright line for hydrogen evolution better than those obtained under aerated conditions.

The potentiodynamic curves at 10°C are not very different from the curves at 20°C. Both the limiting current density (according to Eq. (2)) and the free corrosion potential remain practically unchanged. For the rotating disk electrode, the effects of the increase in oxygen content and of the decrease in mass transport coefficient from 20 to 10°C practically compensate each other. At potentials more negative than -1000 mV (SCE), the curves at 20 and 10°C become significantly different in that the hydrogen evolution seems to occur at more negative potentials as temperature decreases. As far as the analytical expression of the polarization curve is concerned, the Tafel slope, that is the B_H parameter, varies with temperature according to RT/0.5F, while a rough calculation gives the approximate value of 1.4×10^{-14} A/cm^2 for the I_H parameter at 10°C.

CONCLUSIONS

i) The analytical expression:

$$i(A/cm^2) = 1.5 \times 10^{7} \exp(FE/RT) - i_L - 8 \times 10^{-14} \exp(-0.5FE/RT)$$

can describe the cathodic polarization curve of a carbon steel in 3.5% NaCl solution at 20°C in the potential range between -700 and -1200 mV vs SCE.

ii) For the rotating disk electrode the limiting current density for oxygen reduction is given by the expression :

$$Sh = 0.621(1 + 0.298\ Sc^{-1/3} + 0.14514\ Sc^{-2/3})^{-1} . Re^{1/2} . Sc^{1/3}$$

iii) For potential values more positive than -700 mV vs SCE, the above analytical expression does not reproduce the experimental polarization curves and the expected free corrosion potential is 80 mV lower than the experimental one. This is probably due to film formation on the steel. Moreover, the oxygen reduction does not occur under limiting current conditions at these positive potentials. However, such differences can be disregarded because under cathodic protection the steel is polarized at potentials more negative than -800 mV vs SCE. On the contrary, such differences must be taken into account if insufficiently polarized areas are present on the structure, as it could happen during initial polarization.

iv) Decreasing temperature, the hydrogen evolution seems to occur at more negative potential values. The pre-exponential factor I_H (equal to 8×10^{-14} A/cm^2 at 20°C) changes with temperature and becomes about 1.4×10^{-14} A/cm^2 at 10°C.

REFERENCES

1. E.A. Decarlo, Materials Performance, 22, n. 7 (1983) 38
2. R. Strømmen and A. Rødland, Materials Performance, 20, n. 4 (1981) 15
3. J.W. Fu and J.S.J. Chow, Materials Performance, 21, n. 10 (1982) 9
4. A. Turnbull and M.K. Gardner, Corrosion Science, 22 (1982) 661
5. M. Stern, Journal Electrochemical Society, 102 (1955) 609
6. K. Nisancioglu, Paper No. 314, Proceedings Corrosion-85, NACE, Houston (1985)
7. K.F. Sander, Proceedings Conference on Cathodic Protection Theory and Practice - The Present Status, Coventry (1982)
8. B. Mazza, T. Pastore, P. Pedeferri, G. Taccani, E. Ferrari, and F. Gasparoni, Experimental Confirmation of a Mathematical Model for the Design of Cathodic Protection Systems, Proceedings 10th International Congress on Metallic Corrosion, Madras (1987)
9. O.F. Devereux, Corrosion, 35, n. 3 (1979) 125
10. Y. Massiani, J.P.Crousier, J. Crousier, J. Galea, and R. Romanetti, Electrochimica Acta, 29 (1984) 1679
11. R.S. Munn, Materials Performance, 21, n. 8 (1982) 29
12. J.R. Selman and C.W. Tobias, Advances in Chemical Engineering, Ed. Drew et al., Vol. 10, Academic Press, New York (1978) pp. 211-318
13. N. Ibl. and O. Dossenbach, Compre - hensive Treatise of Electrochemistry, Ed. Yeager et al., Vol. 6, Plenum Press, New York (1983) pp. 133-237
14. National Research Council (USA), International Critical Tables, McGraw-Hill, New York (1926-1933)
15. V.Y. Filinovsky and Y.V. Pleskov, Comprehensive Treatise of Electrochemistry, Ed. Yeager et al., Vol. 9, Plenum Press, New York (1984) pp. 293-352